PCCP

Accepted Manuscript

ROYAL SOCIETY OF CHEMISTRY

www.rsc.org/pccp

DFT approach to the Charge Transport Related Properties in Columnar Stacked π-Conjugated N-Heterocycles Cores Including Electron Donor and Acceptor Units

Amparo Navarro,[§] M. Paz Fernández-Liencres,[§] Gregorio García,[‡] José M. Granadino-Roldán,[§] and Manuel Fernández-Gómez[§]*

[§]Departamento de Química Física y Analítica. Facultad de Ciencias Experimentales, Universidad de Jaén. Paraje las Lagunillas, E23071, Jaén, Spain

[‡]Departamento de Química, Universidad de Burgos, Plaza Misael Bañuelos E09001 Burgos, Spain

(*) Corresponding Author: +34-953212148; e-mail address: mfg@ujaen.es

ABSTRACT: We present a density functional theory (DFT) study on charge-transport related properties in a series of discotic systems based on 1,3,5-triazine and tris[1,2,4]triazolo[1,3,5]triazine central cores as electron acceptor units, and phenyl-thiophene and N-carbazolyl-thiophene segments as electron donor units. The presence of both electron

donor and acceptor moieties in the π-conjugated core could lead to new discotic liquid crystals (DLC) materials which are predicted to display ambipolar charge transport behavior in such a way that electrons could move through the central part of the next cores while holes mainly do through the peripheral groups. A significant increase in hole mobility when N-carbazolyl is present as electron donor unit in the peripheral region is predicted. In addition, a detailed topological analysis of the electron charge density within the framework provided by Quantum Theory of Atoms in Molecules (QTAIM) has been performed in order to characterize intra- and intermolecular interactions in terms of hydrogen bonds and/or π…π stacking which contribute to the stabilization of the columnar stack and the helical self-assembly at molecular scale.

Keywords: Ambipolar behavior, discotic systems, theoretical design, AIM analysis

INTRODUCTION

Since the first work published in 1977 by Chandrasekhar et al. about benzene-hexa-n-alkanoates,[1] discotic liquid crystals (DLCs) have attracted a lot of attention due to their properties to form nanostructures with an one-dimensional pathway for charge transport and, thus with interesting applications in organic electronics.[2,3] DLC materials are being recognized as a new class of quality organic semiconductors with mobilities in the range 10^{-4}-1 $cm^2V^{-1}s^{-1}$. The applicability of these materials in optoelectronics as well as the design of new mesogens with improved electronic properties depend on several molecular properties as HOMO/LUMO levels, reorganization energy, integral transfer and π-stacking, among others.[4-30]

They consist of a central π-conjugated core in which the insertion of lateral chains may lead to ordered, columnar mesophases. Specific substitutions on both, the core and side chains may

induce changes in the interdisc, azimuthal angle reducing the steric hindrance and favoring a helical π-stacking along the column as opposite to a face-to-face one. In addition, non-covalent interactions, such as H-bonds and dipole interactions, play an important role in the formation of supramolecular assemblies. As a matter of fact, the role played by specific functional groups on both, the appearance of new inter-disc, non-covalent interactions and charge transport related properties is of high current interest.[21,31-33]

Nowadays there is a huge field of research about organic, narrow band gap polymers with ambipolar charge transport behavior. One way to achieve intrinsic ambipolar charge transport in conjugated linear polymers is through the existence of linked electron-donor and acceptor units in the molecular structure, which has shown to be an efficient strategy to reduce the band gap due to the mixing of molecular segments with higher HOMO and lower LUMO.[34-37] However, the design of processable, ambipolar structures formed by ordered liquid crystals (LC) for optoelectronic applications is still a field to explore and represent a new challenge in the development of novel materials with promising applications as field-effect transistors, light-emitting diodes and photovoltaic cells.[38-51]

Recently, a new series of DLC conducting materials based on octupolar 1,3,5 triazine central cores, as electron acceptor unit, and peripheral, electron donor phenyl-thiophene and N-carbazolyl-thiophene units has been synthesized opening a promising guideline for the design of ambipolar LC materials.[52] Both thiophene and N-carbazolyl have been widely used in electronic devices, and exhibit p-type semiconductor properties.[53-57] However, not many works have been devoted to thiophene [29] or N-carbazolyl [55] based discotic systems. To our knowledge, the first hexagonal columnar DLC carbazole derivative with triphenylene core was synthesized in 2001

by Manickam et al.[55] while their photoconductivity properties were studied in 2007 concluding that these systems behave as p-type semiconductors.[56]

In this work, we present a detailed quantum chemical investigation on the charge transport-related properties of a series of columnar π-stacked acceptor cores based on 1,3,5-triazine linked to peripheral donor segments whose properties as charge transport carriers have shown an ambipolar behavior from time-of-flight measurements (see Chart 1).[52] Moreover, aimed at the design of new ambipolar DLC materials we have studied the effect of modifying the nature of both, the acceptor central core and peripheral donor moieties, on charge transport related properties of a series of compounds based on the tris[1,2,4]triazolo[1,3,5] triazine core (see Chart 1) recently synthesized.[58,59] As said before, interdisc distances and orientations of the stacked cores have a great influence on the charge transport related properties. Hence, characterization at the molecular scale of DLCs is an utmost important issue in the study of charge transport properties of the self-assembled structure and to establish structure-properties relationships.

In order to theoretically discern the suitability of the selected systems, some of them not synthesized yet, as the active part of *n*-, *p*- or ambipolar materials, different properties such as intramolecular reorganization energy, frontier molecular levels, charge carrier mobility and charge transfer integral have been calculated on the basis of density functional theory (DFT). In addition, the intra- and intermolecular interactions, responsible of the stability of DLC columnar mesophases and, then, of their charge transport related properties, have been characterized on the basis of a topological analysis of electron charge density in terms of critical points as Atoms in Molecules Theory deals with.

THEORETICAL METHODOLOGY

Gaussian09 (revision B.01)[60] suite of programs has been mostly employed for the theoretical calculations. In order to assess charge transport related properties for each system under study, we have used different approximations. First, geometries of the neutral and charged, anionic and cationic, molecules of the selected compounds (Chart 1) were fully optimized at the hybrid B3LYP level [61-63] along with 6-31G* basis set.[64] Using these geometries, intramolecular reorganization energies were determined by using B3LYP [61-63] and M06-2X[65] functionals with 6-31G* and 6-311G** basis sets[64] by performing single point calculations. Both functionals have shown to give reasonable values for transfer integrals and non-covalent interactions in previous works.[8,17,21,66] We are aware the best description for anions is expected to be obtained by using diffuse basis sets. However, using the previously mentioned basis sets is expected to render similar results to those obtained when introducing diffuse functions in the basis set.[17, 67, 68]

Second, the columnar stacked π-conjugated cores were modeled by a cluster made up of five molecules. The lateral chains linked to the phenyl or N-carbazolyl rings play an important role in the columnar mesophases stabilization and the relative positions of the disc in the one-dimensional nanostructure. However, as it can be found in the literature, the increase of the chain length has not a great impact on the magnitude of the charge transport related properties such as transfer integrals and reorganization energies and may overshadow the understanding of the intermolecular interactions inside the columnar stacks.[17,29,69] Thus, the calculations have been performed at the molecular level with methyl/methoxy moieties as shown in Chart 1 which also reduces the computational cost compared with more extended alkyl/alkoxy chains.

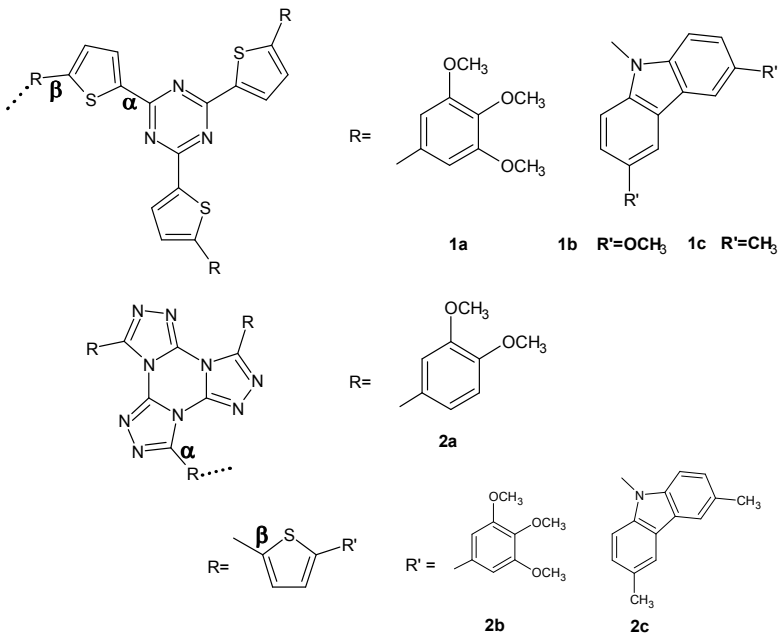

Chart 1. Molecular geometry for the selected compounds

Due to the large number of atoms in the clusters, *ca*. 500-600, their geometries were fully optimized in the context of the two-layer ONIOM model.[70] This method allows for an effective partition of the system in different ("small" and "large") subunits, each of them modeled with an increasing accuracy, usually labeled as "high" and "low" levels (see **Figure 1**).

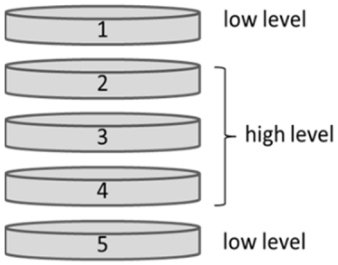

Figure 1. Schematic representation of the cluster

In our systems, for each 5-membered cluster, three inner molecules were studied at PBE/6-31G* [71,72] (high level) while two outer molecules were studied at PBE/STO-3G [64] (low level).

This partition model allows us to optimize a large system, focusing on the central units which are described in a more realistic environment and avoiding the edge effects. Last, although frequently termed "weak," dispersion forces can account for a large percentage of the interaction energy of molecular complexes of modest size. The standard approximations to the exchange-correlation functional of DFT cannot describe the dispersion interaction correctly and thus we have also considered dispersion corrections for PBE functional. We have selected the general chemistry GGA type PBE functional including the so-called Grimme's D2 dispersion correction term, as implemented in Gaussian 09 B.01[60], as it has been proven to perform well for large systems at predicting geometry parameters, ionization potential, electron and proton affinities, as well as for describing van der Waals and hydrogen bond interactions at a reasonable computational cost.[73-77]

The design of the cluster model implies a careful study of three important parameters such as azimuthal angle, inter-core distance and side displacement which, as known, play an important role in the charge transport process. Thus, several papers have appeared dealing with the impact of both the interdisc separation and the azimuthal angle in the charge carrier mobility inside DLC.[8,17,21] The inter-core distance values for semiconducting columnar mesogens are usually in the range 3.5-4.0 Å. For azimuthal angles, a large range of values can be found depending on the core and the lateral chains yielding either face-to-face or helical architectures on the columnar stack.[21]

According to XRD data, the triazine core derivatives selected in this work stack in a helical pattern along the column axis minimizing in this way the steric hindrance of the side chains.[52] A similar result was obtained for tristriazolotriazine core derivative by circular dichroism.[59]

In order to get theoretical information about the most favorable arrangement of the discs inside the cluster, the evolution of the total energy for a couple was calculated as the azimuthal angle varies. The interdisc distance was kept at 3.6 Å since the transfer integral does not show a noticeable sensitivity on this parameter within the range of interest, i.e. 3.5-3.6 Å.[17] **Figure 2** shows the barrier to rotation for a couple made up of two units of 2,4,6-tris(thiophene-2-yl)-[1,3,5]triazine and tris[1,2,4]triazolo[1,3,5] triazine. The most stable arrangement was found for cores rotated each other *ca.* 60^{o} in both cases, in agreement with the experimental findings for the corresponding DLC compounds. When methoxyphenyl moieties were symmetrically linked to the central cores, we obtained a broader well where the steric hindrance among the peripheral segments would be minimized (see **Figure 1S**).

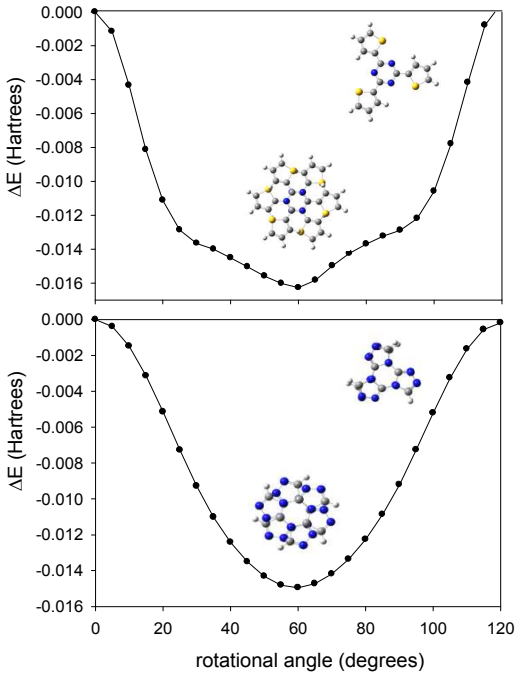

Figure 2. Total energy *vs*. azimuthal angle for a couple of triazine (up) and tristriazolotriazine (down) cores. Intermolecular distance is fixed at 3.6 Å.

According to these results, a five-membered model cluster with an inter-core distance equal to 3.6 Å and a rotational angle of 60º was built up using as starting point the molecular geometry optimized for each molecule at the B3LYP/6-31G* level. Then, the geometry of the cluster was fully optimized through ONIOM approach (see above). The charge transfer integral (*t*) between two molecules in an inner couple within the optimized cluster was estimated following the so-called projective method, using the code *J-from-g03*.[78,79] Hole and electron mobilities were evaluated through the charge transfer rate k_{ET} calculated according to Marcus-Levitch-Jortner theory.[80-83]

Finally, in order to analyze intra- (from one isolated molecule) and intermolecular interactions (from a couple of two consecutive or alternate molecules), the topological analysis of the electronic charge density was performed within the Quantum Theory of Atoms in Molecules (QTAIM) with AIM2000 program package.[84,85]

RESULTS AND DISCUSSION.

Molecular geometry. **Table 1** gathers the α and β dihedral angles (see Chart 1) for the selected compounds at the B3LYP/6-31G* level. X-ray data for *1a* and *2a* establish α dihedral angle in the range 1-11º [52] and 19-62º [58], respectively. The discrepancy with the B3LYP/6-31G* value for *2a*, i.e. ~ 28º, could be due, as will be discussed later, to the stacking of the molecules. As seen from β values, the N-carbazolyl derivative deviates more from planarity in order to decrease the steric hindrance which could limit strongly any mixing between the molecular orbitals of thiophene and N-carbazolyl units. Also, β dihedral angle appears to be strongly influenced by the charge located on the system. This will show up in the corresponding reorganization energies.

Table 1. Mean torsional angles α and β (in degrees) at the B3LYP/6-31G* level**.**

		1a	**1b**	**1c**	**2a**	**2b**	**2c**
α(N-C-C-S/C)	neutral	1.0	1.1	0.3	28.0	1.2	0.9
	cation	0.2	0.6	0.3	19.1	0.7	0.5
	anion	0.7	0.1	0.1	11.4	0.3	0.6
β(S-C-C/N -C)	neutral	27.6	50.5	51.7		26.1	52.2
	cation	19.3	46.7	48.0		15.0	45.4
	anion	17.1	74.7	78.7		12.4	70.4

The large deviation from planarity could prevent π-stacking along the column and, at the same time, give rise to non-covalent interactions among neighbor discs leading to an enhanced columnar organization. Thus, in order to understand the spreading of co-planarity between the central core and the peripheral units we characterized first the interatomic interactions within each single disc on the basis of Bader's topological analysis of the charge electron density, ρ_b.[85] (See supplementary information for details and **Figure 2S**). Accordingly, Table **1S** lists the values for the topological parameters of the Bond Critical Points (BCP) for each single disc at the B3LYP/6-31G* level. All the interactions fall into the closed-shell type and they are associated to intramolecular H-bonds as they fulfill the topological criteria proposed by Koch and Popelier. [86,87] $C_{thiophene}\cdots H_{carbazol}$, $S_{thiophene}\cdots H_{carbazol}$, $N_{triazol}\cdots H_{phenyl}$ and $N_{triazol}\cdots H_{thiophene}$ intramolecular contacts were found which enhances the planarity of the core and hinders the rotation of the lateral segments. **Figure 3** shows the intramolecular contacts found in the case of the *2c* compound.

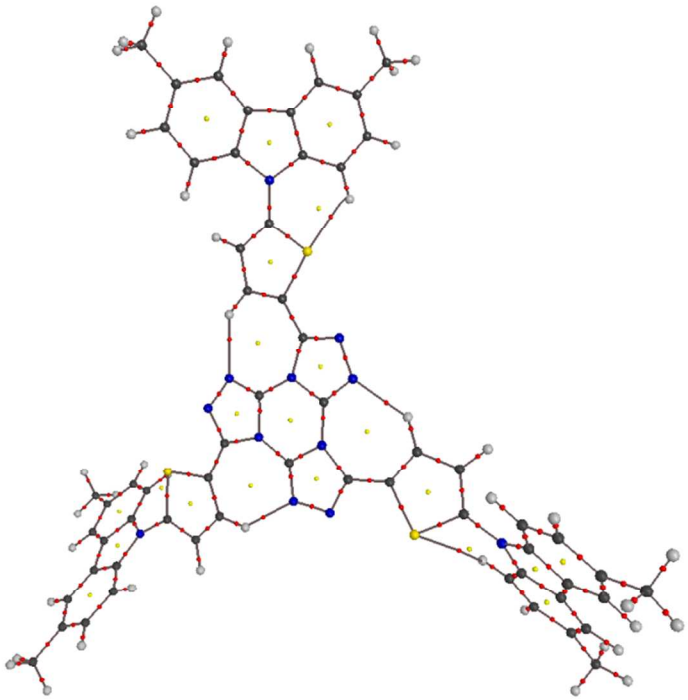

Figure 3. Molecular graph for *2c*. Keys for atoms: black = C, red = O, blue = N, gray = H. Small dots represent CPs: red = BCP, yellow = RCP.

According to $|V_b|/G_b$ and bond-degree (BD) H_b/ρ_b indexes (see Supplementary information for details and **Figures 3S** and **4S**), the S···H and N···H contacts, mainly accounting for the spreading of the planarity from the central cores to the peripheral groups, turn out to be the weaker and the stronger, respectively. Therefore, it could be expected that at least the N···H contacts would remain when they enter into the cluster.

Cluster geometry. The clusters present a π-stacking arrangement typical for a hexagonal, helical coil, minimizing the steric hindrance among the side chains. This result matches the experimental findings for triazine and tristriazolotriazine derivatives.[52,59] In **Figure 4** an upper view of the optimized structure for each cluster is shown.

Table 2 shows that α dihedral angle for *1a-c* and *2b-c* is close to the values in the single molecules. However, the β dihedral angle is smaller in the cluster than in the single molecules, except for *2c*. This effect could be due to the flattening packing effect of the molecules in the columnar stack. The largest deviation from planarity is found for *1b*, *1c* and *2c* which may favor a *non* face-to-face packing in order to reduce the peripheral steric hindrance. As a result, a number of intermolecular contacts among neighboring, nearly parallel N-carbazolyl rings may appear.

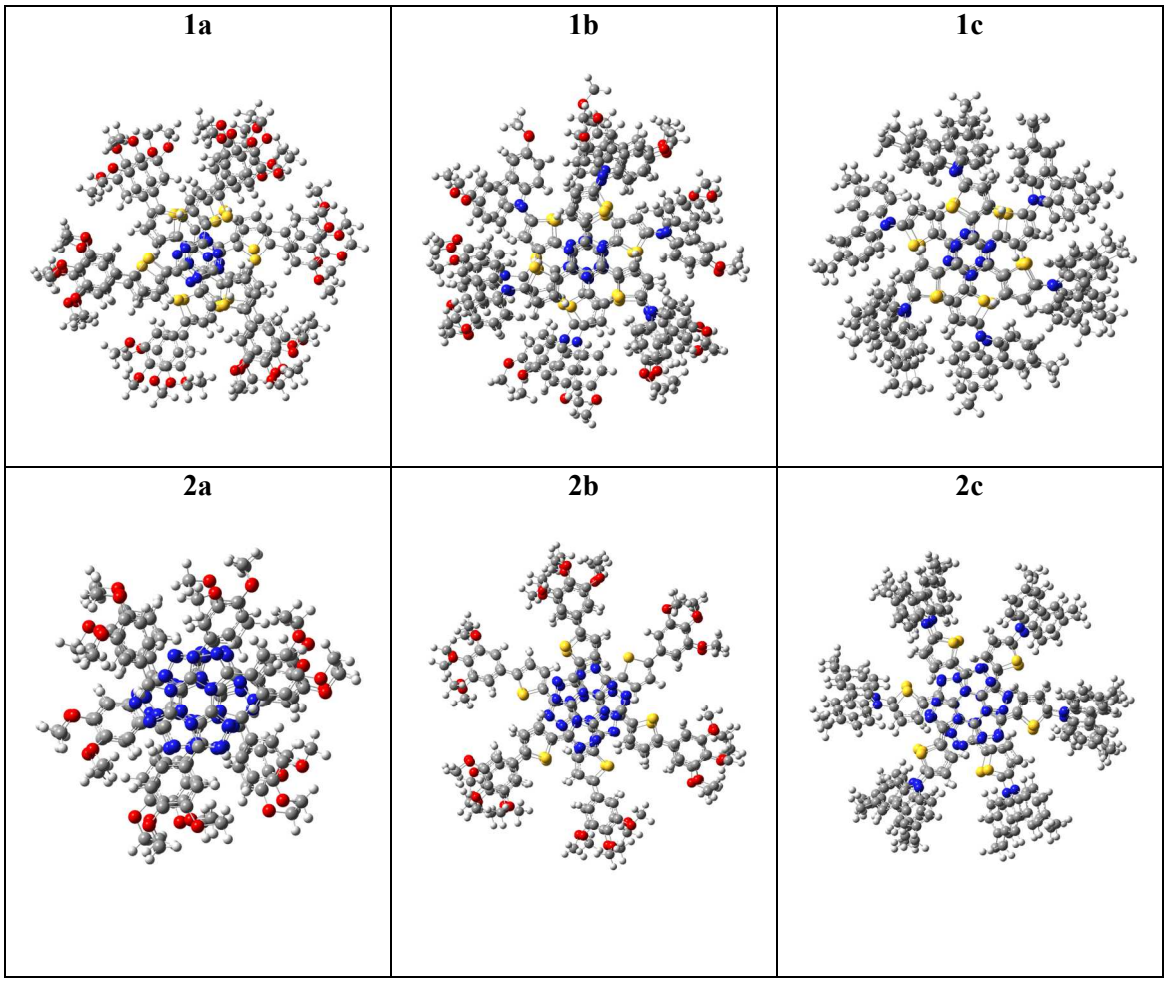

Figure 4. Upper view of the optimized structures for the five-membered clusters (white: H; grey: C red: O; yellow: S; blue: N).

For clustered *2a*, the three α-type torsional angles become clearly different each other at odds with those shown by the isolated molecule in agreement with a previous X-ray study.[58] The inter-core distances predicted for a clustered, central couple as well as those from an X-ray analysis are collected in **Table 2**.[52,59] Both sets of data are similar but far from the typical value for such a parameter in semiconducting DLCs (~ 3.5-4.0 Å). The shortening of the inter-core distance from *2a* to *2c* may be due to the intermolecular contacts the thiophene ring can give rise as a consequence of the higher facility to accommodate the peripheral segments in the helical columnar stacking.

Table 2. Mean torsional angles, α and β (in degrees), for the central molecule in the cluster and interdisc distance (in Å) at PBE/6-31G* level.*

	1a	**1b**	**1c**	**2a**	**2b**	**2c**
α(N-C-C-S/C)	1.4	1.4	2.9	20.4 28.8 38.1	0.7	0.9
β(S-C-C/N -C)	24.6	43.3	39.0	-	25.2	54.6
$d(C_{core}-C_{core})$	3.1(3.3)[a]	3.1	3.2	3.3(3.5)[b]	3.2	3.1

*X-Ray experimental data in parenthesis.
[a] ref.52; [b] ref.59.

Inter- and intramolecular, non-covalent interactions may contribute to enhance the intracolumnar order.[33] As those contacts can be of different nature and/or magnitude, here we have performed a QTAIM analysis on couples of discs either consecutive (2,3) and alternate (2,4) in order to characterize the different contacts not only in terms of covalent interactions but

also in terms of H-bonds and π…π stacking ones as it has been already described in the literature.[88,89] The results appear in **Tables 3** and **1S**. The contacts can be classified as closed-shell interactions as they all present positive values for $\nabla^2\rho_b$ and H_b. **Figure 5S** show a schematic representation of the BCPs for the different couples. Some more detailed comments about the AIM results for intramolecular H-bond interactions can be seen in the Supplementary information.

In general, intramolecular H-bonds in the couples are slightly shorter than in their corresponding single units with higher values for ρ_b and $\nabla^2\rho$ pointing to an increase of the bond strength. As expected, the AIM analysis of the intermolecular interactions becomes more complex due to intermolecular contacts are found not only between the conjugated central cores of neighboring discs but also between the peripheral segments in all the selected compounds.

Several intermolecular H-bonds in (2,4) and (2,3) couples are found between neighboring cores which could stabilize the helical disposition of the discs along the column. In addition,π…π stacking interactions between both the central part of the cores and the N-carbazolyl groups could play an important role in that stabilization. The core enlargement renders an increase in the number of π…π stacking contacts. In addition, a significantly higher number of intermolecular interactions are found in clusters with peripheral N-carbazolyl moieties as compared to those with methoxyphenyl (see **Table 3**).

Table 3. Bond distances, electron density and Laplacian for Bond Critical Points for intermolecular interactions in the selected cluster at the B3LYP/6-31G* level.

Cluster	Couple	Bond (A···B)	distance (Å)	ρ_b (au)	$\nabla^2\rho_b$ (au)
1a	2,4	H_{meth}···H_{meth}	2.222	0.007	0.0255

	2,3	$O_{meth}\cdots H_{meth}$	2.429	0.011	0.039
		$C_{meth}\cdots H_{meth}$	2.736	0.007	0.028
		$C_{triaz}\cdots C_{triaz}$	3.061-3.088	0.008	0.029-0.030
1b	2,4	$O_{meth}\cdots H_{meth}$	2.439-2.757	0.006-0.010	0.025-0.035
		$C_{carb}\cdots H_{meth}$	2.558-2.763	0.008-0.010	0.031-0.035
		$C_{carb}\cdots O_{meth}$	3.120-3.128	0.008	0.027-0.028
		$C_{carb}\cdots C_{carb}$	3.217	0.008	0.025
	2,3	$S_{thio}\cdots H_{thio}$	2.963	0.008	0.027
		$H_{thio}\cdots H_{carb}$	2.116-2.840	0.006-0.009	0.027-0.034
		$C_{thio}\cdots H_{carb}$	2.562-2.621	0.009-0.010	0.035-0.037
		$S_{thio}\cdots C_{thio}$	3.167-3.245	0.010-0.012	0.032-0.039
		$C_{triaz}\cdots N_{triaz}$	3.106-3.116	0.008	0.026-0.027
1c	2,4	$H_{methyl}\cdots H_{methyl}$	2.228	0.008	0.027
		$C_{methyl}\cdots H_{methyl}$, $C_{carb}\cdots H_{methyl}$	2.613-2.828	0.007-0.010	0.024-0.032
		$C_{carb}\cdots C_{carb}$	3.182-3.369	0.007-0.008	0.024-0.026
	2,3	$H_{thio}\cdots H_{carb}$	2.148-2.294	0.007-0.010	0.029-0.040
		$C_{carb}\cdots H_{carb}$	2.723	0.009	0.029
		$S_{thio}\cdots C_{thio}$	3.055-3.331	0.009-0.014	0.027-0.045
		$C_{triaz}\cdots N_{triaz}$	3.151	0.008	0.025
2a	2,4	$O_{meth}\cdots H_{meth}$	2.577	0.007	0.027
		$H_{meth}\cdots H_{meth}$	2.263	0.008	0.030
	2,3	$N_{triazol}\cdots H_{phenyl}$	2.519-2.551	0.010-0.011	0.039-0.042
		$H_{phenyl}\cdots H_{phenyl}$, $H_{phenyl}\cdots H_{meth}$, $H_{meth}\cdots H_{meth}$	2.102-2.266	0.007-0.010	0.028-0.039
		$C_{triaz}\cdots N_{triaz}$, $C_{triaz}\cdots N_{triazol}$	3.179-3.194	0.007	0.024
2b	2,4	$H_{meth}\cdots H_{meth}$	2.295	0.006	0.022
	2,3	$C_{triaz}\cdots N_{triaz}$	3.130-3.193	0.007-0.008	0.025-0.028
		$C_{triazol}\cdots N_{triazol}$	3.128-3.146	0.007-0.008	0.025-0.026
		$C_{thio}\cdots N_{triazol}$	3.096	0.009	0.026
2c	2,4	$C_{carb}\cdots H_{methyl}$	2.736-2.788	0.007-0.008	0.025-0.027
		$C_{carb}\cdots C_{carb}$	3.088-3.299	0.008-0.010	0,023-0.030
	2,3	$C_{triaz}\cdots N_{triaz}$	3.090-3.097	0.009	0.029
		$C_{triazol}\cdots N_{triazol}$	3.124-3.180	0.007-0.008	0.024-0.026

*subscripts "*thio*", "*carb*" "*triazol*" and "*triaz*" stand for thiophene, carbazolyl, triazolyl and triazine, respectively.

A molecular graph of intra- and intermolecular contacts for the (2,4) and (2,3) couples in *2c* is shown in **Figures 5** and **6**, respectively. The AIM results for the rest of the clusters concerning BCPs associated to the closed-shell interactions can be seen in Supplementary Material (**Table 1S**). For couple (2,4), six BCPs associated to $C_{carb}\cdots C_{carb}$ interactions, a large number of RCPs and, finally, six CCPs between the N-carbazolyl units can be seen in **Figure 5**. This result suggests the dominant interaction is the π…π stacking along with peripheral $C_{carb}\cdots H_{methyl}$ H-bond (see **Table 1S**). These ones are also observed in the couple (2,4) for *1c*.

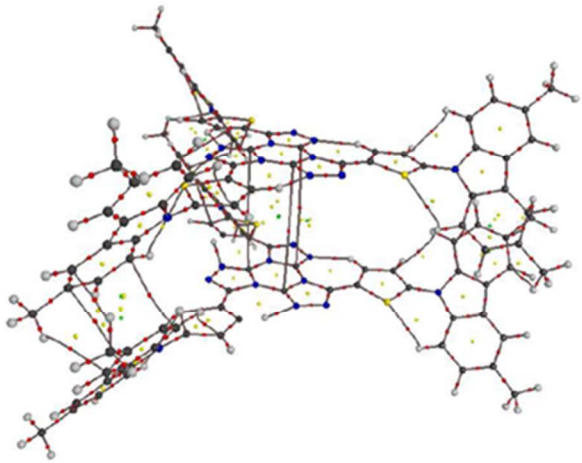

Figure 5. Molecular graph of couple (2,4) for *2c*. (black=C, red=O, blue=N, grey=H). Small dots mean Critical Points (CPs): red= BCP, yellow= RCP, green= Cage Critical Point (CCP).

For couple (2,3), eleven BCPs associated to $C_{triaz}\cdots N_{triaz}$ interactions in *2c* (see **Table 1S**), three RCPs and seven CCPs between the tristriazolotriazine central cores (see **Figure 6**) are found whereas no intermolecular interactions between the N-carbazolyl segments appear. Therefore

π…π stacking become the only dominant interactions in the (2,3) couple and, in general, play an important role in the stabilization of the *2c* cluster.

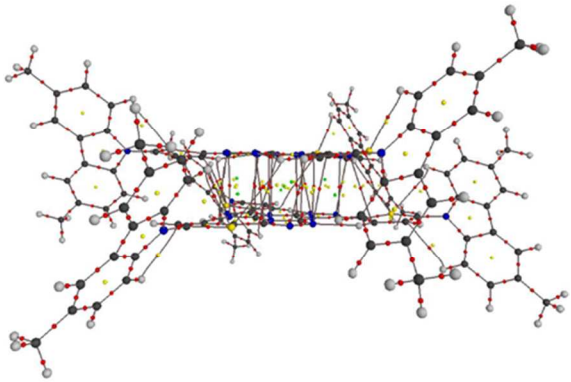

Figure 6. Molecular graph of couple (2,3) for *2c*. (black=C, red=O, blue=N, grey=H). Small dots represent CPs: red=BCP, yellow=RCP, green=CCP.

The intermolecular contacts between either consecutive (2,3) and alternate (2,4) units through H-bonds and/or π…π stacking interactions favor the helical disposition of the discs along the column. However, the core-peripheral intramolecular interactions could force the structure of the discs to flatten favoring their stacking and they could prevent the formation of intermolecular contacts between two adjacent discs. Therefore, the balance between intra and intermolecular interactions is an important issue to be considered when designing new core molecular structures for DLC purposes.

Charge injection. HOMO/LUMO levels, electron affinity and ionization potential are the main parameters controlling the efficiency of charge injection. Although different models for charge injection from the metal electrode into the semiconductor organic material have been proposed theoretically and investigated from an experimental point of view, it is generally accepted that the energy gap between the work function of the electrode, Φ_m, and the LUMO/HOMO of the semiconductor rules the efficiency for electron/hole injection into the

active material.[90-92] Koopmans' theorem states that in closed-shell Hartree-Fock theory the first (gas phase) ionization potential, IP, equals to minus the HOMO energy. Although it could be argued that Koopmans' theorem is not applicable to Kohn-Sham orbital energies, Janak's theorem provides a link between frontier orbital energies and ionization potential (IP) and electron affinities (EA), as well.[93]

For an efficient hole/electron injection, suitable HOMO/LUMO levels and low/high IPs/EAs are desirable. However, low IPs would lead to unintentional doping, and therefore to low ON/OFF ratios,[94] and EA higher than 4.0 eV could result in a too electrophilic molecule which could be unstable in ambient conditions.[93] LUMO and HOMO frontier orbitals of the studied compounds are shown in **Figure 7**. As it can be seen, the HOMO is mainly located on the peripheral, electron donor region, while the LUMO is expanded over the central, electron acceptor region of the cores. As described above, the electron donor groups become closer to each other in couple (2,4) increasing HOMO overlap and then the hole transport. Thus, the electron mobility is facilitated by the overlap between the LUMO orbitals of the electron acceptor units (triazine and tristriazolotriazine cores) while the hole transport would mainly occur through the donor, peripheral groups (phenyl-thiophene and N-carbazolyl-thiophene). Taking into account the helical disposition of the molecules within the columnar stack and the shape of HOMO and LUMO orbitals shown in **Figure 7**, this could result in two main channels for charge transport: holes could mainly move through the peripheral groups and electrons do through the central part of the neighboring cores.

Table 4 gathers the theoretical HOMO/LUMO energies along with the experimental band gaps. As it can be seen, B3LYP and M06-2X functionals predict HOMO-LUMO energy gaps wider than the experimental ones, although B3LYP behaves better than M06-2X, regardless of

the basis set. Notwithstanding, these values are one order of magnitude larger than those ones previously reported for ambipolar conjugated polymers.[37,51]

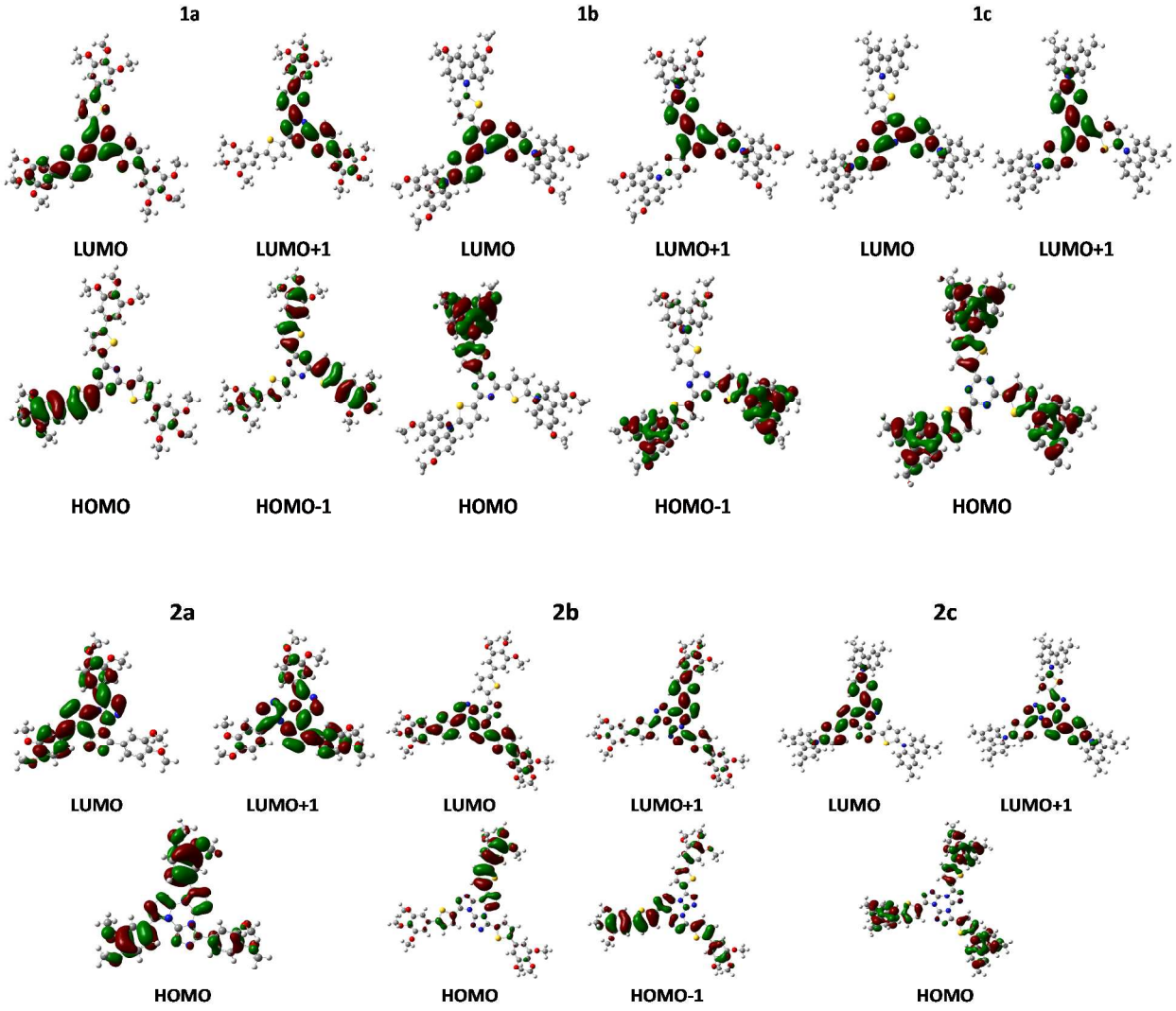

Figure 7. HOMOs and LUMOs contours for the selected compounds at the B3LYP/6-31G* level.

Narrow bandgaps are needed in order to design ambipolar materials. One strategy to get this in semiconducting polymers is to alternate electron donor and accepting units. In this work, a decrease of *ca.* 1.0 eV is observed when we compare the calculated E_g value for *2a* with those for *2b* and *2c*. In addition, the bandgap also decreases around 0.3 eV when the phenyl-thiophene

is changed by N-carbazolyl-thiophene. As a matter of fact, the narrowest band gaps are predicted for *1b*, *1c* and *2c*.

Table 4. Theoretical and experimental energy values (eV) for the HOMO and LUMO levels and band gap.

		1a	1b	1c	2a	2b	2c
B3LYP/6-31G*	LUMO	-1.9216	-1.9687	-2.0607	-1.5118	-2.0150	-2.0767
	HOMO	-5.4794	-5.0019	-5.3178	-5.8223	-5.5581	-5.3553
	E_g	3.56	3.03	3.26	4.31	3.54	3.28
B3LYP/6-311G**	LUMO	-2.1684	-2.2062	-2.2623	-1.7401	-2.2416	-2.2914
	HOMO	-5.7074	-5.2372	-5.5327	-6.0489	-5.7823	-5.5869
	E_g	3.54	3.03	3.27	4.31	3.54	3.30
M06-2X/6-311G**	LUMO	-1.4522	-1.4786	-1.5086	-0.8514	-1.4550	-1.4656
	HOMO	-6.9883	-6.4653	-6.7259	-7.1076	-7.0345	-6.7787
	E_g	5.54	4.99	5.22	6.26	5.58	5.31
Exp.	E_g	2.56[ξ]		2.37[ξ]	3.56*		

[ξ]Ref. 52. Experimental data from ref.33 in CH_2Cl_2 solution.

* Ref.59. Optical value for the energy gaps from film absorption spectra.

Finally, as seen in **Table 4**, the E_g predicted for *1a* and *2b* as well as for *1c* and *2c* suggests that the substitution of triazine by tristriazolotriazine in the core does not affect significantly to the bandgap energies. A word of caution must be said here. Comparison between experimental values of E_g for (*1a*, *1c*) and *2a* may be strongly influenced by the very different dielectric constant of CH_2Cl_2 solutions for the former and that of thin film for the latter.

Figure 8 renders the theoretical HOMO/LUMO energy levels of the studied compounds along with the work function Φ_m of common electrodes.[90-92] An ohmic contact is achieved when the energy differences are less than 0.3 eV.[90] According to Cristiano et al.[59], *2a* should behave as an electron-transporting system while as seen in **Figure 8**, the highest LUMO energy is predicted for it. B3LYP predicts *2c* to show the lowest LUMO energy, even though it is still far from the

cathode work functions herein shown. As a general trend, a decrease in LUMO energies is predicted when going from *1a* to *1b*-*1c*, and also from *2a* to *2b*-*2c*. This points out that sticking phenyl- and N-carbazolyl-thiophene groups to the tristriazolotriazine core produces a significant decrease of the LUMO energy level (~0.5 eV). This decrease is also observed when the phenyl groups are substituted by N-carbazolyl units in both series of studied compounds, although the effect is less pronounced (0.1 eV). For *1b*, HOMO energy is closer to $\Phi_{m,ITO}/\Phi_{m,Au}$ than *1a* and *1c* and then an easier hole injection should be expected.

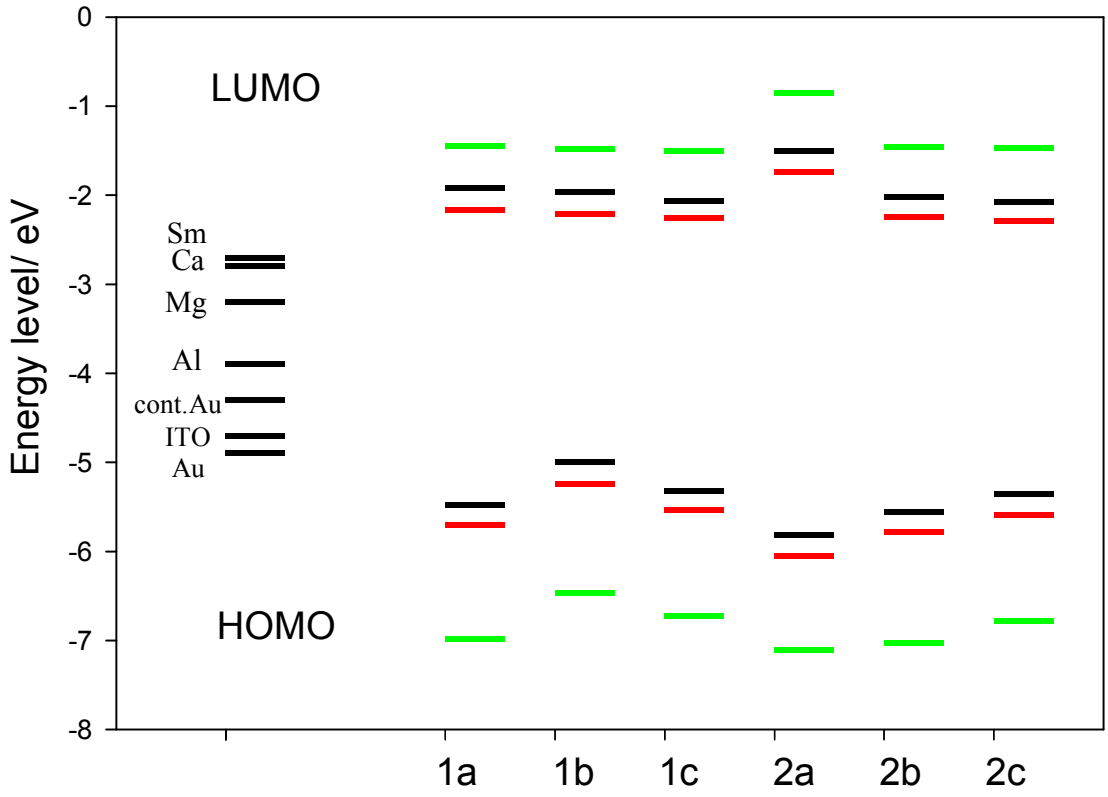

Figure 8. HOMO and LUMO energy levels (eV). (green**:** M06-2X/6-311G**;** red**:** B3LYP/6-311G**;** black: B3LYP/6-31G*).

Also, Φ_m-$|E_{HOMO}|$< 0.3 eV and then an ohmic contact could be possible. In addition, HOMO energy for *2c* is higher than those of *2b* and *2a*, and close to that for *1c*. As a general trend N-carbazolyl unit in the peripheral region produces an increasing of the HOMO energy, in agreement with the *p* character of this substituent.

Another important issue when studying charge injection are the adiabatic, electron affinity (AEA) and ionization potential (AIP) as they must be high/low enough to allow an efficient electron/hole injection into the LUMO/ HOMO level (see **Table 5)**.

Table 5. Intramolecular hole (λ_+) and electron (λ-) reorganization energies, adiabatic ionization potential (AIP) and electron affinities (AEA) (units in eV) at different levels of theory.

	Method	λ_+	AIP	λ-	AEA
1a	B3LYP/6-31G*	0.588	5.95	0.301	1.03
	B3LYP/6-311G**	0.593	6.19	0.300	1.26
	M06-2X/6-311G**	0.707	7.02	0.341	1.16
1b	B3LYP/6-31G*	0.096	5.96	0.443	1.39
	B3LYP/6-311G**	0.096	5.74	0.449	1.11
	M06-2X/6-311G**	0.114	5.54	0.463	1.49
1c	B3LYP/6-31G*	0.059	6.77	0.421	1.31
	B3LYP/6-311G**	0.059	5.49	0.413	1.45
	M06-2X/6-311G**	0.072	6.06	0.472	1.17
2a	B3LYP/6-31G*	0.553	6.28	0.510	1.46
	B3LYP/6-311G**	0.553	5.92	0.505	1.58
	M06-2X/6-311G**	0.620	7.04	0.576	1.38
2b	B3LYP/6-31G*	0.365	6.26	0.219	1.16
	B3LYP/6-311G**	0.362	6.48	0.164	1.32
	M06-2X/6-311G**	0.573	7.23	0.266	1.07
2c	B3LYP/6-31G*	0.076	6.05	0.305	1.21
	B3LYP/6-311G**	0.074	6.28	0.297	1.45
	M06-2X/6-311G**	0.082	7.09	0.370	1.19

Figure 9 shows that the predicted AEA values are less sensitive to the theoretical method than AIP ones. When phenyl-thiophene is changed by N-carbazolyl-thiophene in both series *1* and *2*, a decrease of AIP is predicted at B3LYP/6-311G** and M06-2X/6-311G** levels yielding the lowest values for *1c* (B3LYP/6-311G**) and *1b* (M06-2X/6-311G**). However, B3LYP/6-31G* predicts an increase when going from *1a* to *1c*. **Figure 9** also shows that the highest AEA is found for *2a* at B3LYP. This result agrees with Cristiano et al.[59] who suggest the potential electron-transporting character of tristriazolotriazine which could be facilitated by a high AEA.

However, when thiophene is added to the tristriazolotriazine central core, the AEA decreases and takes values close to those for the triazine case**.**

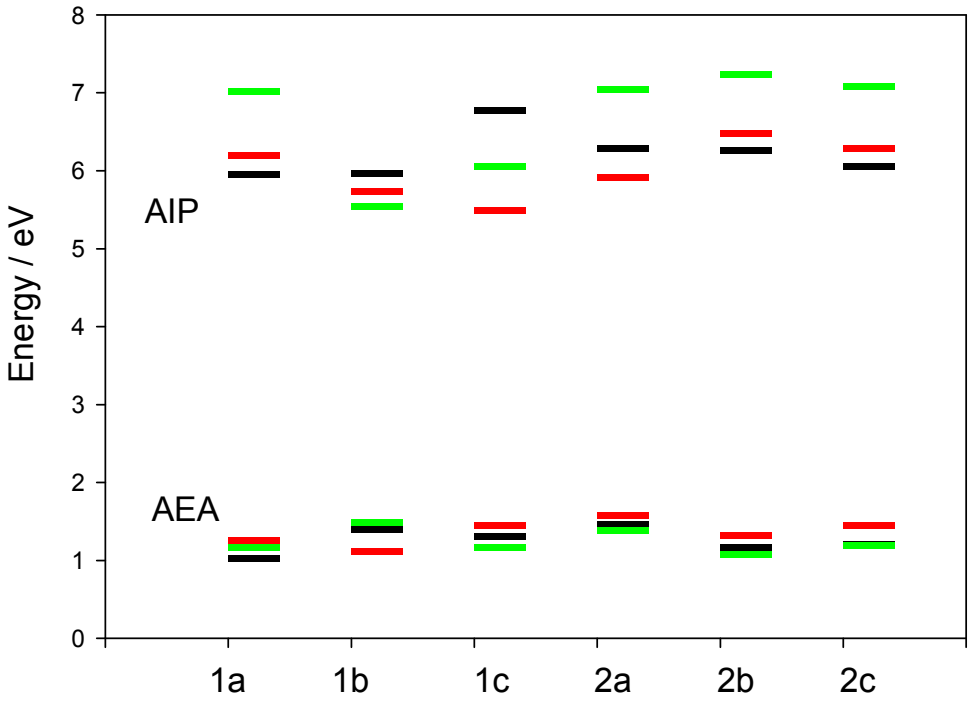

Figure 9. Calculated AIPs and AEAs for the selected systems at different levels of theory (green: M06-2X/6-311G**; red: B3LYP/6-311G**; black: B3LYP/6-31G*).

Therefore, as a general trend, N-carbazolyl-thiophene segments induce both higher/lower AEA/AIP and HOMO/LUMO energy level compared with methoxyphenyl, and then it could be considered as a suitable electron donor unit in searching for new, ambipolar materials when nitrogen rich central cores, as triazine and tristriazolotriazine, act as electron acceptor units.

Charge Carrier Mobility. Charge transport within discotic phase mainly occurs by a hopping regime. The charge hopping process could be defined as a self-exchange, charge-transfer

reaction between two molecules. The non-adiabatic intermolecular charge transfer rate with vibronic corrections upon mode averaging is given by the Marcus-Levich-Jortner model [80,81]

$$k_{ET} = \frac{2\pi}{\hbar} t^2 \sqrt{\frac{1}{4\pi\lambda_0 k_B T}} \sum_{n=0}^{\infty} \left[exp\left(-S_{eff}^n\right) \times \frac{S_{eff}^n}{n!} \times exp\left(\frac{-\left(\lambda_0 + n\hbar\omega_{eff} + \Delta G^0\right)^2}{4\lambda_0 k_B T} \right) \right] \quad (1)$$

In this expression t is the charge transfer integral (electronic coupling), ΔG^0 is the energy difference between the electronic states involved in the charge transfer process (equal to zero in the self-exchange process), $S_{eff} = \lambda_{int}/\hbar\omega_{eff}$ is the effective Huang-Rhys factor, related to both λ_{int}, the internal reorganization energy mainly determined by fast changes in molecular geometry, and ω_{eff}, the frequency of the effective vibrational mode assisting the process (fixed at ~1600 cm^{-1}, the breathing mode of aromatic rings, *i.e.* $\hbar\omega_{eff} \sim 0.2$ eV) and λ_o is the classical (mostly the external) contribution to the reorganization energy.[95-99]

Unlike ions migration in mesophase materials, the electronic charges, i.e. electron and holes, are transported via a rigid solid-like region consisting of closely packed π-conjugate core moiety of liquid crystalline molecules. As we are interested in electronic transport along the column, we disregard the contribution of the solvation term to the reorganization energy[47] and we consider the outer contribution to the reorganization energy as due to the nuclear relaxation of the environment caused by electronic polarization.[100]

The microscopic evaluation of the external reorganization energy is a difficult task [94] and that is the reason why not many papers devoted to deal with have been published so far.[100,101] Thus, it is often considered as a tunable parameter.[68,97,102] A typical value in the range 0.1-0.2 eV is generally adopted.[96, 99] In this work, we have adopted the value 0.15 eV as a reasonable one for

materials with a certain degree of short-range order [68,97,98] and it is also within the range 0.1x-2x the internal reorganization energy whatever the compound selected.[103]

It must be taken into account that λ_{ext} might depend on the molecular environment. Hence, assuming an unique, fixed value for it could influence the reliability of the final results. The expected non-very different polarizability of the studied compounds, however, may reinforce such a choice[101] bearing in mind that the final interest of the paper is not to obtain absolute values of mobilities but rather to outline trends along the series of the selected compounds.

According to the hopping mechanism, the drift mobility (μ_{hop}) and the diffusion coefficient (D) are related by the Einstein relation[104]

$$\mu_{hop} = \frac{eD}{k_B T} \qquad (2)$$

where T is the temperature, k_B is the Boltzmann constant and for a one-dimensional system, where only one neighbor is considered, D is given by $D = ½\ l^2 K_{ET}$ where l is the hopping distance.[105] It must be said that this model gives values for transfer rates and carrier mobilities which must only be considered as superior and ideal limits.[106,107] Internal reorganization energy is related to the delocalized nature of the HOMO/LUMO and for an isolated molecule consists of the sum of two terms: $\lambda = \lambda_1 + \lambda_2$, where λ_1 and λ_2 can be calculated directly from the adiabatic potential energy surface as:

$$\lambda_{total}^{\pm} = \lambda_1^{\pm} + \lambda_2^{\pm}$$

$$\lambda_1^{\pm} = E_{\pm}(G_N) - E_{\pm}(G_{\pm})$$

$$\lambda_2^{\pm} = E_N(G_{\pm}) - E_N(G_N)$$

where (N, +/-) denote neutral and charged states, respectively; $E_N(G_N)$ and $E_\pm(G_\pm)$ are the ground-state energies of the neutral and charged states, respectively while $E_N(G_\pm)$ and $E_\pm(G_N)$ are the energies of the neutral molecule at the optimal charged geometry and the energy of the charged state at the optimal geometry of the neutral molecule, respectively. The calculated reorganization energies λ_i for the selected compounds are shown in **Table 5**.

As can be seen, M06-2X yields higher λ_i values for both the negative and positive polarons while the effect of the basis set is almost negligible for B3LYP, with the exception of λ_- for *2b*.

The comparison of the theoretical values for the selected compounds with those previously calculated for other typical DLCs shows that both electron and hole reorganization energies are the same order of magnitude.[18,26,108] For comparison purposes, from now on we will restrict our discussion to the results obtained at B3LYP level.

As a general trend, $\lambda_+(\lambda_-)$ decreases(increases) when phenyl-thiophene is changed by N-carbazolyl-thiophene ~ 0.4(0.1) eV. This effect is observed when the central core is triazine (*1b* and *1c*) and also tristriazolotriazine (*2b* and *2c*). Also, λ_+ values predicted for *1b*, *1c* and *2c* are in the range 0.06-0.1 eV, and they are similar to those calculated for triphenylene (0.18 eV), HATNA (0.14 eV) and HBC (0.10 eV) at the B3LYP/6-31G** level by Lemaur et al.[17]

Compound *2a* shows $\lambda_{+/-}$ which are 0.18/0.29 eV higher than those for *2b*. In addition, when methoxyphenyl is changed in *2b* by N-carbazolyl to give *2c*, λ_- remains almost constant although λ_+ decreases dramatically up to 0.47 eV from *2a*. As a result, the increase in size of the central core and the number of nitrogen atoms when going from *1a* to *2b*, keeping the same peripheral group, produces a significant decrease of λ_+ (λ_-) around 0.22 eV (0.1 eV). In addition λ_+ and λ_-

become smaller when the substituent in the N-carbazolyl is methyl (*1c*) instead of methoxyphenyl (*1b*).

The smallest λ_-'s are obtained for *2b*, *2c* and *1a*. They are in the range 0.22-0.30 eV and close to those calculated for triphenylene (0.26 eV) and HAT (0.27 eV)[17] and slightly higher than those for electron rich oligoacenes (~ 0.10 eV),[109] HATNA (0.10 eV) and HBC (0.14 eV).[17]

Despite λ_i and *t* can be calculated separately, it is necessary to calculate charge mobility as a function of both parameters to conclude about the *p*-, *n*- or ambipolar character of these compounds.

In **Table 6** $t_{+/-}$ and $\mu_{+/-}$ values are listed for the compounds studied in this work. As the ratio μ_+/μ_- points out, a *p*-type semiconductor behavior in varying degrees should be expected in most cases regardless of the couple, (2,3) or (2,4), dealt with. Electron transport, however, mainly occurs between successive discs as it is the case for *1a* and *1c*. Due to the less effective overlap of the peripheral groups between successive discs, hole transport occurs not only through (2,3) couple, but also between two alternate discs, the latter becoming dominant in *1a-c* and *2c*. This is a consequence of the location of the HOMO/LUMO orbitals and the helical position of the cores as described above.

Hole mobility in (2,3) couple for *1a* ($\mu_+ \sim 10^{-6}$ cm^2 V^{-1} s^{-1}) is much lower than the electron one ($\mu_- \sim 10^{-1}$ cm^2 V^{-1} s^{-1}) due to the less effective overlap of the phenyl-thiophene segments, which is increased between two alternate units ($\mu_+ \sim 10^{-3}$ cm^2 V^{-1} s^{-1}), in reasonable agreement with values from TOF data.[52] Thus, experimental $\mu_{-/+}$ values for a compound similar to *1a* but with side -$OC_{12}H_{25}$ chains were *ca*. 4.10^{-3} /3.10^{-5} cm^2 V^{-1} s^{-1} in Col_h phases.[52] As expected, there is not

quantitative agreement between the theoretical and experimental values due to neglect the stack dynamics calculating the mobility, but the theoretical results keep a similar trend.

For *1c* no distinct electron mobility could be determined from the experimental measurements,[52] although the authors predicted a μ_+ value larger than that for *1a*, ~ 1.10^{-3} cm^2 V^{-1} s^{-1} in Col_h phases with $-OC_{12}H_{25}$ as side chain. As seen in **Table 6**, values for μ_+ for *1a* and *1c* in the (2,4) couples follow the same trend while *1b* keeps values larger than those for *1a* and *1c*, *i.e.* $\mu_+(1a) << \mu_+(1b) > \mu_+(1c)$. As for μ_- it drops abruptly when going either from *1a* and *1c* to *1b* both for (2,3) and (2,4) couples.

Table 6. Calculated transfer integral t (eV) and mobility μ ($cm^2V^{-1}s^{-1}$) for holes and electrons.

	Method	Couple	t_+	t_-	μ_+	μ_-
1a	B3LYP/6-31G*	2,3	$6.58.10^{-5}$	$8.68.10^{-2}$	$4.33.10^{-8}$	$3.16.10^{-1}$
	B3LYP/6-311G**		$1.86.10^{-3}$	$7.41.10^{-2}$	$3.38.10^{-5}$	$2.03.10^{-1}$
	M06-2X/6-311G**		$6.66.10^{-3}$	$9.16.10^{-2}$	$2.44.10^{-4}$	$2.87.10^{-1}$
	B3LYP/6-31G*	2,4	$4.50.10^{-3}$	$2.74.10^{-3}$	$8.11.10^{-4}$	$1.25.10^{-3}$
	B3LYP/6-311G**		$6.37.10^{-3}$	$4.20.10^{-3}$	$1.58.10^{-3}$	$2.97.10^{-3}$
	M06-2X/6-311G**		$5.44.10^{-3}$	$5.32.10^{-3}$	$6.52.10^{-4}$	$3.97.10^{-3}$
1b	B3LYP/6-31G*	2,3	$1.35.10^{-2}$	$1.04.10^{-2}$	$2.15.10^{-2}$	$2.23.10^{-3}$
	B3LYP/6-311G**		$1.31.10^{-2}$	$5.58.10^{-3}$	$2.03.10^{-2}$	$6.28.10^{-4}$
	M06-2X/6-311G**		$1.57.10^{-2}$	$8.73.10^{-3}$	$2.66.10^{-2}$	$1.44.10^{-3}$
	B3LYP/6-31G*	2,4	$1.95.10^{-2}$	$2.71.10^{-3}$	$1.79.10^{-1}$	$6.12.10^{-4}$
	B3LYP/6-311G**		$2.05.10^{-2}$	$3.36.10^{-3}$	$1.98.10^{-1}$	$9.14.10^{-4}$
	M06-2X/6-311G**		$2.35.10^{-2}$	$4.61.10^{-3}$	$2.38.10^{-1}$	$1.60.10^{-3}$
1c	B3LYP/6-31G*	2,3	$1.63.10^{-2}$	$1.00.10^{-1}$	$3.85.10^{-2}$	$2.37.10^{-1}$
	B3LYP/6-311G**		$1.36.10^{-2}$	$1.18.10^{-1}$	$2.66.10^{-2}$	$3.44.10^{-1}$
	M06-2X/6-311G**		$8.60.10^{-3}$	$1.50.10^{-1}$	$1.00.10^{-2}$	$4.14.10^{-1}$
	B3LYP/6-31G*	2,4	$1.09.10^{-2}$	$4.84.10^{-3}$	$6.90.10^{-2}$	$2.22.10^{-3}$
	B3LYP/6-311G**		$1.34.10^{-2}$	$4.35.10^{-3}$	$1.04.10^{-1}$	$1.86.10^{-3}$
	M06-2X/6-311G**		$1.54.10^{-2}$	$4.51.10^{-3}$	$1.28.10^{-1}$	$1.50.10^{-3}$
	B3LYP/6-31G*	2,3	$6.99.10^{-2}$	$3.87.10^{-2}$	$6.36.10^{-2}$	$2.42.10^{-2}$
	B3LYP/6-311G**		$6.85.10^{-2}$	$3.85.10^{-2}$	$6.11.10^{-2}$	$2.45.10^{-2}$
	M06-2X/6-311G**		$7.22.10^{-2}$	$5.17.10^{-2}$	$4.86.10^{-2}$	$3.11.10^{-2}$
	B3LYP/6-31G*		$9.07.10^{-3}$	$3.93.10^{-4}$	$4.29.10^{-3}$	$9.97.10^{-6}$

2a	B3LYP/6-311G**	2,4	$8.20.10^{-3}$	$8.19.10^{-4}$	$3.50.10^{-3}$	$4.44.10^{-5}$
	M06-2X/6-311G**		$5.07.10^{-3}$	$1.01.10^{-3}$	$9.60.10^{-4}$	$4.74.10^{-5}$
2b	B3LYP/6-31G*	2,3	$4.75.10^{-2}$	$2.33.10^{-2}$	$7.30.10^{-2}$	$3.64.10^{-2}$
	B3LYP/6-311G**		$5.08.10^{-2}$	$2.01.10^{-2}$	$8.49.10^{-2}$	$3.58.10^{-2}$
	M06-2X/6-311G**		$5.77.10^{-2}$	$2.41.10^{-2}$	$3.80.10^{-2}$	$3.07.10^{-2}$
	B3LYP/6-31G*	2,4	$4.88.10^{-3}$	$1.12.10^{-4}$	$2.89.10^{-3}$	$3.15.10^{-6}$
	B3LYP/6-311G**		$5.79.10^{-3}$	$3.79.10^{-4}$	$4.14.10^{-3}$	$4.77.10^{-5}$
	M06-2X/6-311G**		$5.77.10^{-3}$	$1.94.10^{-5}$	$1.43.10^{-3}$	$7.52.10^{-8}$
2c	B3LYP/6-31G*	2,3	$2.51.10^{-2}$	$4.21.10^{-2}$	$8.09.10^{-2}$	$7.28.10^{-2}$
	B3LYP/6-311G**		$2.84.10^{-2}$	$5.42.10^{-2}$	$1.05.10^{-1}$	$1.25.10^{-1}$
	M06-2X/6-311G**		$3.05.10^{-2}$	$5.35.10^{-2}$	$1.16.10^{-1}$	$8.46.10^{-2}$
	B3LYP/6-31G*	2,4	$1.13.10^{-1}$	$2.84.10^{-3}$	6.53	$1.33.10^{-3}$
	B3LYP/6-311G**		$1.23.10^{-1}$	$3.41.10^{-3}$	7.81	$1.98.10^{-3}$
	M06-2X/6-311G**		$1.33.10^{-1}$	$4.76.10^{-3}$	8.83	$2.68.10^{-3}$

The higher μ_+ in *1c* as compared to *1a* could be due to the enhanced HOMO overlap when the N-carbazolyl is in the peripheral region, which is less effective in *1a*.[52] On the other hand, mobilities in *1a* and *1c* are comparable to those observed for several DLCs as Cu-phthalocyanine derivatives ($\mu_- = 2.4.10^{-3}$ $cm^2V^{-1}s^{-1}$; $\mu_+ = 2.17.10^{-3}$ $cm^2V^{-1}s^{-1}$),[45] HDBP-3 ($\mu_- \approx \mu_+ \sim 10^{-3}$ $cm^2V^{-1}s^{-1}$),[43] HT5 ($\mu_- \approx \mu_+ \sim 10^{-3}$ $cm^2V^{-1}s^{-1}$), HT6 ($\mu_- \approx \mu_+ \sim 10^{-4}$ $cm^2V^{-1}s^{-1}$) and HHTT ($\mu_- \approx \mu_+ \sim 10^{-3}$ $cm^2V^{-1}s^{-1}$), [50] among others.

For tristriazolotriazine core derivatives, the experimental data point out that *2a* could potentially present electron transport properties, although data for mobility have not been reported.[59] For *2a* in the (2,3) couple, theoretical values for μ_+ and μ_- turn out to be similar each other, but smaller than μ_- for *1a*. Therefore, the two dimensional expansion of the conjugated core does not seem to play any significant role in improving electron mobility.

For *2a* and *2b*, calculations predict similar values for μ_- and slightly lower than that for *2c* in (2,3) couple. In addition, μ_- for *2c* is lower than that for *1a* and *1c*, while μ_+ becomes clearly

larger than that for *1b* and *1c*. As to (2,4) couple, μ_+ for *2c* turns out to be nearly two orders of magnitude larger than that for *1c*. This fact could be due to the higher overlap of the N-carbazolyl units in *2c* which renders larger values for t_+ being λ_+ nearly the same in both systems. Furthermore, despite the distance between central cores in (2,4) couple is about double that for the (2,3) one, the distance between the N-carbazolyl planes of two (2,4) discs keeps about 3.8 Å, and then, a higher μ_+ could be obtained if it is considered for *l* in equation (2).

The relative mobility μ_-/μ_+ for (2,3) couple clearly points out that *1a* presents larger electron mobility than the hole one, in agreement with the experimental data,[52] as well as *1c*, while the opposite behavior is found for *1b* regardless of the couple, *i.e.* (2,3) or (2,4), μ_+ refers to. For *2a* and *2b*, hole mobility is larger than the electron one, especially for (2,4) couple while for *2c* the ratio μ_-/μ_+ keeps nearly unity for (2,3) couple. Finally, the relative mobilities, $\mu/\mu_{(1a)}$ keep greater than unity for hole mobility regardless of the couple considered while for electron mobility the ratio keeps lower than unity except for *1c* for which a more balanced situation is shown.

Therefore, the new, not synthesized yet molecules, *2b* and *2c*, are predicted to yield values for charge transport related properties in the same range of those for *1a* and *1c*, for which ambipolar character has been proven, and thus they could be considered reasonable candidates for ambipolar DLC materials.

CONCLUSIONS

Our theoretical study has allowed us to reproduce the relative values for the electron and hole mobilities of the ambipolar compounds *1a* and *1c*, in agreement with the experimental data.

Atoms-in-Molecules (AIM) analysis concludes that core enlargement renders an increase in the number of π…π stacking contacts and the intermolecular contacts between either consecutive (2,3) and alternate (2,4) units through H-bonds and/or π…π stacking interactions favor the helical disposition of the discs along the column. Core-peripheral intramolecular interactions could force the structure of the discs to flatten favoring their stacking. However, they could prevent the formation of intermolecular contacts between two adjacent discs. Therefore, in order to get stable columnar mesophases when designing new DLCs the competition between inter- and intramolecular interactions should be carefully considered.

In order to interpret the ambipolar charge transport behavior of those compounds, the existence of two main charge transport channels has been proposed, one for the hole transport through the HOMO orbitals located in the peripheral region where the phenyl-thiophene or N-carbazolyl-thiophene segments are present, and another one for electron transport through the LUMO orbitals, located in the central region of the core where the triazine or tristriazolotriazine are present. Furthermore, we have predicted the hole and electron mobilities for two new compounds, named *2b* and *2c*, which have not been synthesized yet. The last one has shown a significant increase of the hole mobility due to the presence of the N-carbazolyl unit. From a theoretical point of view, the intrinsic nature of these compounds has proven they are good candidates for ambipolar charge transport, and this feature could play an important role in their applications as organic semiconductors in the future.

ASSOCIATED CONTENT

Supporting Information. Comments on the QTAIM analysis, Rotational barrier for the couple of 1a and 2a at B3LYP/6-31G* level, Representation of the intramolecular bond paths in

single molecules of the selected compounds, Dependence of $|V_b|/G_b$ and H_b/ρ_b indexes on the interatomic distance, Representation of the inter and intra molecular bond paths for the (2,4) couples and Topological properties for single disc and (2,3) and (2,4) couples at the B3LYP/6-31G* level.

AUTHOR INFORMATION

Corresponding Author

* E-mail: mfg@ujaen.es .

ACKNOWLEDGEMENT

Support from Consejería de Innovación, Ciencia y Empresa, Junta de Andalucía, Spain (PAI-FQM- 337 grant) and Centro Informático Científico de Andalucía is gratefully acknowledged.

REFERENCES

1 S. Chandrasekhar, B. K. Sadashiva, K. A. Suresh, *Pramana*, 1977*,* **9***,* 471 - 480.

2 M. O'Neill, S. M. Kelly, *Adv. Mater*., 2011, **23**, 566 - 584.

3 E. Moulin, J. J. Cid, N. Giuseppone, *Adv. Mater*., 2013, **25**, 477 - 487.

4 V. Coropceanu, J. Cornil, J.; D. A. da Silva Filho, Y. Olivier, R. Silbey, J. L. Brédas, *Chem. Rev*., 2007, **107**, 926 - 952.

5 S. Sergeyev, W. Pisula, Y. H. Geerts, *Chem. Soc. Rev*., 2007, **36,** 1902 - 1929.

6 X. Feng, V. Marcon, W. Pisula, M. Ryan-Hansen, J. Kirkpatrick, F. Grozema, D. Andrienko, K. Kremer, K. Müllen, *Nat. Mater.*, 2009, **8**, 421 - 426.

7 K. Pieterse, P. A. van Hal, R. Kleppinger, J. A. J. M. Vekemans, R. A. J. Janssen, E. W. Meijer, *Chem. Mater.*, 2001, **13**, 2675 - 2679.

8 K. Senthilkumar, F. C. Grozema, F. M. Bickelhaut, L. D. A. Siebbeles, *J. Chem. Phys*., 2003, **119**, 9809 – 9817.

9 J. Cornil, V. Lemaur, J. P. Calbert, J. L. Brédas, *Adv. Mater.*, 2002, **14**, 726 – 729.

10 R. I. Gearba, M. Lehmann, J. Levin, D. A. Ivanov, M. H. J. Koch, J. Barberá, M. G. Debije, J. Piris, Y. H. Geerts, *Adv. Mater*., 2003, **15**, 1614 – 1618.

11 O. D. Jurchescu, J. Bass, T. T. M. Palstra, *Appl. Phys. Lett*., 2004, **84**, 3061 – 3063.

12 D. A. da Silva Filho, E.-G. Kim, J. L. Brédas, *Adv. Mater*., 2005, **17**, 1072 - 1076.

13 R. Juarez, M. Moreno-Oliva, M. Ramos, J. Segura, C. Aleman, F. Rodríguez-Ropero, D. Curco, F. Montilla, V. Coropceanu, J. L. Brédas, *Chem.Eur. J*., 2011, **17**, 10312 - 10322.

14 M. Lehmann, G. Kestemont, R. Gómez Aspe, C. Buess-Herman, M. H. J. Koch, M. G. Debije, J. Piris, M. P. de Haas, J. M. Warman, M. D. Watson, V. Lemaur, J. Cornil, Y. H. Geerts, R. Gearba, D. A. Ivanov, *Chem. Eur. J*., 2005, **11**, 3349 - 3362.

15 B. R. Kaafarani, T. Kondo, J. S. Yu, Q. Zhang, D. Dattilo, C. Risko, S. C. Jones, S. Barlow, B. Domercq, F. Amy, A. Kahn, J. L. Brédas, B. Kippelen, S. Marder, *J. Am. Chem. Soc*., 2005, **127**, 16358 - 16359.

16 X. Crispin, J. Cornil, R. Friedlein, K. K. Okudaira, V. Lemaur, A. Crispin, G. Kestemont, M. Lehmann, M. Fahlman, R. Lazzaroni, Y. Geerts, G. Wendin, N. Ueno, J. L. Brédas, W. R. Salaneck, *J. Am. Chem. Soc*., 2004, **126**, 11889 - 11899.

17 V. Lemaur, D. A. da Silva Filho, V. Coropceanu, M. Lehmann, Y. Geerts, J. Piris, M. G. Debije, A. M. van de Craats, K. Senthilkumar, L. D. A. Siebbeles, J. M. Warman, J. L. Brédas, J. Cornil, *J. Am. Chem. Soc*., 2004, **126**, 3271 - 3279.

18 M. G. Debije, J. Piris, M. P. de Hass, J. M. Warman, Z. Tomovic, C. D. Simpson, M. D. Watson, K. Müllen, *J. Am. Chem. Soc*., 2004, **126**, 4641 - 4645.

19 Y. Olivier, V. Lemaur, J. L. Brédas, J. Cornil, *J. Phys. Chem. A*, 2006, **110**, 6356 - 6364.

20 G. Cinacchi, G. Prampolini, *J. Phys. Chem. C*, 2008, **112**, 9501 - 9509.

21 W. Pisula, X. Feng, K. Müllen, *Adv. Mater*., 2010, **22**, 3634 - 3649.

22 A. Demenev, S. H. Eichhorn, T. Taerum, D. F. Perepichka, S. Patwardhan, F. C. Grozema, L. D. A. Siebbeles, *Chem. Mater*., 2010, **22**, 1420 - 1428.

23 L. Wang, G. Nan, X. Yang, Q. Peng, Q. Li, S. Zhigang, *Chem. Soc. Rev*., 2010, **39**, 423 - 434.

24 J. E. Anthony, A. Facchetti, M. Heeney, S. R. Marder, X. Zhan, *Adv. Mater*., 2010, **22**, 3876 - 3892.

25 L. A. Haverkate, M. Zbiri, M. R. Johnson, B. Deme, M. Fokko, F. M. Mulder, G. J. Kearley, *J. Phys. Chem. B*, 2011, **115**, 13809 - 13816.

26 B. R. Kaafarani, *Chem. Mater.*, 2011, **23**, 378 - 396.

27 W. Pisula, X. Feng, K. Müllen, *Chem. Mater.*, 2011, **23**, 554 - 567.

28 L. Lin, H. Geng, Z. Shuai, Y. Luo, *Org. Electron.*, 2012, **13**, 2763 - 2772.

29 G. García, M. Moral, J. M. Granadino-Roldan, A. Garzón, A. Navarro, M. Fernández-Gómez, *J. Phys. Chem. C*, 2013, **117**, 15 - 22.

30 S. Sanyal, A. K. Manna, S. K. Pati, *J. Phys. Chem. C*, 2013, **117**, 825 - 836.

31 F. C. Grozema, L. D. A. Siebbeles, *Int. Rev. Phys. Chem.*, 2008, **27**, 87 - 138.

32 C. Lavigueur, E. J. Foster, V. E. Williams, *J. Am. Chem. Soc*., 2008, **130**, 11791 - 11800.

33 A. Rochefort, E. Bayard, S. Hadj-Messaoud, *Adv. Mater*., 2007, **19**, 1992 - 1995.

34 G. García, M. Moral, A. Garzón, J. M. Granadino-Roldán, A. Navarro, M. Fernández-Gómez, *Org. Electron.*, 2012, **13**, 3244 - 3253.

35 U. Purushotham, G. N. Sastry, *Phys. Chem. Chem. Phys.*, 2013, **15**, 5039 - 5048.

36 S. Akoudad, J. Roncali, *Chem. Commun*., 1998, **19**, 2081 - 2082.

37 T. T. Steckler, X. Zhang, J. Hwang, R. Honeyager, S. Ohira, X.-H. Zhang, A. Grant, S. Ellinger, S. A. Odom, D. Sweat, D. B. Tanner, A. G. Rinzler, S. Barlow, J. L. Brédas, B. Kippelen, S. R. Marder, J. R. Reynolds, *J. Am. Chem. Soc*., 2009, **131**, 2824 - 2826.

38 W. Pisula, A. Menon, M. Stepputat, I. Lieberwirth, U. Kolb, A. Tracz, H.Sirringhaus, T. Pakula, K. Müllen, *Adv. Mater.*, 2005, **17**, 684 - 689.

39 H. Hayashi, W. Nihashi, T. Umeyama, Y. Matano, S. Seki, Y. Shimizu, H. Imahori, *J. Am. Chem. Soc*., 2011, **133**, 10736 - 10739.

40 M. Funahashi, J.-I. Hanna, *Appl. Phys. Lett.*, 2000, **76**, 2574 - 2576.

41 M. Funahashi, J.-I. Hanna, *Appl. Phys. Lett.*, 1998, **73**, 3733 - 3735.

42 M. Funahashi, J.-I. Hanna, *Appl. Phys. Lett.*, 1997, **71**, 602 - 604.

43 L.-Y. Chen, F.-H. Chien, Y.-W. Liu, W. Zheng, C.-Y. Chiang, C.-Y. Hwang, C.-W. Ong, Y.-K. Lan, H. C. Yang, *Org. Electron.*, 2013, **14**, 2065 - 2070.

44 H. Iino, J.-I. Hanna, D. Haarer, *Phys. Rev. B*, 2005, **72**, 193 - 203.

45 H. Fujikake, T. Murashige, M. Sugibayashi, K. Ohta, *Appl. Phys. Lett*., 2004, **85**, 3474 - 3476.

46 S. Méry, D. Haristoy, J .F. Nicoud, D. Guillon, S. Diele, H. Monobec, Y. Shimizuc, *J. Mater. Chem*., 2002, **12**, 37 - 41.

47 H. Iino, J.-I. Hanna, *Opto-Electron. Rev.*, 2005, **13**, 295 - 302.

48 G. Saranya, N. Santhanamoorthi, P. Kolandaivel, K. Senthilkumar, *Int. J. Quantum Chem*., 2012, **112**, 713 - 723.

49 J. Hanna, A. Ohno, H. Iino, *Thin Solid Films*, 2014, **554**, 58 - 63.

50 H. Iino, Y. Takayashiki, J.-I. Hanna, R. J. Bushby, D. Haarer, *Appl. Phys. Lett.*, 2005, **87**, 192105.

51 Z. Chen, M. J. Lee, R. S. Ashraf, Y. Gu, A.-S. Sebastian, M. M. Nielsen, B. Schroeder, T. D. Anthopoulos, M. Heeney, I. McCulloch, H. Sirringhaus, *Adv. Mater*., 2012, **24**, 647 - 652.

52 T. Yasuda, T. Shimizu, F. Liu, G. Ungar, T. Kato, *J. Am. Chem. Soc.*, 2011, **133**, 13437 - 13444.

53 G. García, J. M. Granadino-Roldán, A. Garzón, M. Moral, T. Peña-Ruiz, A. Navarro, M. P. Fernández-Liencres, M. Fernández-Gómez, *J. Phys. Chem. C*, 2010, **114**, 12325 - 123.

54 G. García, A. Garzón, J. M. Granadino-Roldán, M. Moral, M. P. Fernández-Liencres, A. Navarro, M. Fernández-Gómez, *Aust. J. Chem*., 2010, **63**, 1297 - 1306.

55 M. Manickam, M. Belloni, S. Kumar, S. K. Varshney, D. S. S. Rao, P. R. Ashton, J. A. Preece, N. Spencer, *J. Mater. Chem.*, 2001, **11**, 2790 - 2800.

56 M. J. Sienkowska, H. Monobe, P. Kaszynski, Y. Shimizu, *J. Mater. Chem.*, 2007, **17**, 1392 - 1398.

57 B. R. Kaafarani, A. O. El-Ballouli, R. Trattnig, A. Fonari, S. Sax, B. Wex, C. Risko, R. S. Khnayzer, S. Barlow, D. Patra, T. V. Timofeeva, E. J. W. List, J. L. Brédas, S. R. Marder, *J. Mater. Chem. C*, 2013, **1**, 1638 - 1650.

58 R. Cristiano, H. Gallardo, A. J. Bortoluzzi, I. H. Bechtold, C. E. M. Campos, R. L. Longo, *Chem. Commun*., 2008, **41**, 5134 - 5136.

59 R. Cristiano, J. Eccher, I. H. Bechtold, C. N. Tironi, A. A. Vieira, F. Molin, H. Gallardo, *Langmuir*, 2012, **28**, 11590 - 11598.

60 M. J. Frisch et al. *Gaussian 09*, Revision B.01, Gaussian, Inc.: Wallingford, CT 2009.

61 A. D. Becke, *J. Chem. Phys.*, 1993, **98**, 5648 - 5652.

62 C. Lee, W. Yang, R. G. Parr, *Phys. Rev. B*, 1988, **37**, 785 - 789.

63 B. Miehlich, A. Savin, H. Stoll, H. Preuss, *Chem. Phys. Lett*., 1989, **157**, 200-206.

64 W. J. Hehre, L. Radom, P. v. R. Scheleyer, J. A. Pople, *Ab initio Molecular Orbital Theory*; Wiley: New York, 1986.

65 Y. Zhao, D. G. Truhlar, *Theor. Chem. Acc*., 2008, **120**, 215-241.

66 E. G. Hohenstein, S. T. Chill, C. D. Sherrill, *J. Chem. Theory Comput*., 2008, **4**, 1996 – 2000.

67 K. A. McGarry, W. Xie, C. Sutton, C. Risko, Y. Wu, V. G. Jr. Young, J. L. Brédas, C. D. Frisbie, C. J. Douglas, *Chem. Mater.*, 2013, **25**, 2254–2263.

68 J. Idé, R. Mereau, L. Ducasse, F. Castet, Y. Olivier, M. Martinelli, J. Cornil, D. Beljonne, *J. Phys. Chem. B*, 2011, **115**, 5593 – 5603.

69 A. Demenev, S. H. Eichhron, T. Taerum, D. F. Perepichka, S. Patwardhan, F. C. Grozema, L. D. A. Siebbeles, R. Klenkler, *Chem. Mater.*, 2010, **22**, 1420–1428.

70 F. Maseras, K. Morokuma, *J. Comput. Chem*., 1995, **16**, 1170 – 1179.

71 J. P. Perdew, K. Burke, M. Ernzerhof, *Phys. Rev. Lett.*, 1996, **77**, 3865 – 3868.

72 J. P. Perdew, K. Burke, M. Ernzerhof, *Phys. Rev. Lett*., 1997, **78**, 1396.

73 S. Grimme, *J. Comput. Chem*., 2006, **27**, 1787 – 1799.

74 X. Xua, W. A. Goddard III, *J. Chem. Phys*., 2004, **121**, 4068 - 4082.

75 S. Grimme, *J. Comput. Chem*., 2004, **25**, 1463 – 1473.

76 M. Swart, M. Solá, F. M. Bickelhaupt, *J. Comput. Methods Sci. Eng*., 2009, **9**, 69 – 77.

77 T. Le Bahers, M. Rerat, P. Sautet, *J. Phys. Chem. C*, 2014, **118**, 5997 − 6008.

78 B. Baumeier, J. Kirkpatrick, D. Andrienko, *Phys. Chem. Chem. Phys.*, 2010, **12**, 11103 - 11113.

79 J. Kirkpatrick, *Int. J. Quantum Chem*., 2008, **108**, 51 – 56.

80 R. A. Marcus, *Rev. Mod. Phys.*, 1993, **65**, 599 - 610.

81 P. F. Barbara, T. J. Meyer, M. A. Ratner, *J. Phys. Chem.*, 1996, **100**, 13148 -13168.

82 V. Balzani, A. Juris, S. Campagna, S. Serroni, *Chem. Rev.*, 1996, **96**, 759 – 834.

83 J. L. Brédas, J. P. Calbert, D. A. da Silva Filho, J. Cornil, *Proc. Natl. Acad. Sci. U.S.A*., 2002, **99**, 5804 - 5809.

84 F. Biegler-König, J. Schönbohm, D. Bayles, *J. Comput. Chem.*, 2001, **22**, 545 – 559.

85 R. F. W. Bader, *Atoms in Molecules: A Quantum Theory*, Clarendon Press, Oxford, 1990.

86 U. Koch, P. L. A. Popelier, *J. Phys. Chem*., 1995, **99**, 9747 – 9754.

87 P. L. A. Popelier, *J. Phys. Chem. A*, 1998, **102**, 1873 - 1878.

88 M. P. Waller, A. Robertazzi, J. A. Platts, D. E. Hibbs, P. A. William, *J. Comput. Chem*., 2006, **27**, 491-504.

89 R. G. A. Bone, R. F. W. Bader, *J. Phys. Chem*., 1996, **100**, 10892 – 10911.

90 C. R. Newman, C. D. Frisbie, D. A. da Silva Filho, J. L. Brédas, P. C. Ewback, K. R. Mann, *Chem. Mater.*, 2004, **16**, 4436-4451.

91 L. Lindell, A. Burquel, F. L. E. Jakobsson, V. Lemaur, M. Gerggren, R. Lazzaroni, J. Cornil, W. R. Salaneck, X. Crispin, *Chem. Mater*., 2006, **18**, 4246 - 4252.

92 C. K. Chen, L. Y. Zou, S. Huang, C. G. Min, A. M. Ren, J. K. Feng, C. C. Sun, *Org. Electron.*, 2011, **12**, 1198 - 1210.

93 E. Jansson, P. C. Jha, H. Ågren, *Chem. Phys*., 2006, **330**, 166 - 171.

94 L. Reséndiz, M. Estrada, A. Cerdeira, B. Iñiguez, M. J. Deen, *Org. Electron.*, 2010, **11**, 1920 - 1927.

95 J. Kirkpatrick, V. Marcon, J. Nelson, K. Kremer, D. Andrienko, *Phys. Rev. Lett.*, 2007, **98**, 227402 - 227405.

96 Y. Geng, J. Wang, S. Wu, H. Li, F. Yu, G. Yang, H. Gao, Z. Su, *J. Mater. Chem*., 2011, **21**, 134 - 143.

97 J. Idé, R. Méreau, L. Ducasse, F. Castet, H. Bock, Y. Olivier, J. Cornil, D. Beljonne, G. D'Avino, O.M. Roscioni, L. Muccioli, C. Zannoni, *J. Am. Chem. Soc*., 2014, **136**, 2911 - 2920.

98 E. Di Donato, R. P. Fornari, S. Di Motta, Y. Li, Z. Wang, F. Negri, *J. Phys. Chem. B*, 2010, **114**, 5327 – 5334.

99 Y. Olivier, L. Muccioli, V. Lemaur, Y. H. Geerts, C. Zannoni, J. Cornil, *J. Phys. Chem. B*, 2009, **113**, 14102 – 14111.

100 J. E. Norton, J. L. Brédas, *J. Am. Chem. Soc*., 2008, **130**, 12377–12384.

101 P. McMahon, A. Troisi, *J. Phys. Chem. Lett*., 2010, **1**, 941 – 946.

102 Y.-F. Chang, Z.-Y. Lu, L.-J. An, J.-P. Zhang, *J. Phys. Chem. C*, 2012, **116**, 1195 -1199.

103 S. E. Koh, C. Risko, D. A. da Silva Filho, O. Kwon, A. Facchetti, J. L. Brédas, T. J. Marks, M. A. Ratner, *Adv. Funct. Mater.*, 2008, **18**, 332 – 340.

104 P. Pope, C. E. Swenberg, *Electronic Process in Organic Crystals and Polymers, 2nd ed*., Oxford, New York, 1999.

105 S. Wen, A. Li, J. Song, W. Deng, K. Han, W. A. Goddard III, *J. Phys. Chem. B*, 2009, **113**, 8813 – 8819.

106 V. Rühle, A. Lukyanov, F. May, M. Schrader, T. Vehoff, J. Kirkpatrick, B. Baumeier, D. Andrienko, *J. Chem. Theory Comput.* 2011, **7**, 3335 – 3345.

107 A. Troisi, *Chem. Soc. Rev*., 2011, **40**, 2347 – 2358.

108 S. Barlow, Q. Zhang, B. R. Kaafarani, C. Risko, F. Amy, C. K. Chan, B. Domercq, Z. A. Starikova, M. Y. Antipin, T. V. Timofeeva, B. Kippelen, J. L. Brédas, A. Kahn, S. R. Marder, *Chem. Eur. J.*, 2007, **13**, 3537 – 3547.

109 M. Winkler, K. N. Houk, *J. Am. Chem. Soc*., 2007, **129**, 1805 – 1815.